2004

Simulation of An Innovative Rotary Compressor With Variable Speed Displacers

A. R. Barreto
Pontíficia Universidade Católica do Rio de Janeiro

Julio Kopelowicz
Dalvic Comercio e Industria Ltd

Jose A. R. Parise
Pontíficia Universidade Católica do Rio de Janeiro

SIMULATION OF AN INNOVATIVE ROTARY COMPRESSOR WITH VARIABLE SPEED DISPLACERS

A.R. Barreto[1], H. J. Kopelowicz[2], J.A.R. Parise[1]

[1] Pontifical Catholic University of Rio de Janeiro, Department of Mechanical Engineering,
22453-900 Rio de Janeiro, RJ, Brazil
Phone: (+5521) 3114 1308; Fax: (+5521) 3114 1309;
andre@visualnet.com.br; parise@mec.puc-rio.br *(corresponding author)*

[2] Dalvic Comércio e Indústria Ltda.
20220-330 Rio de Janeiro, RJ, Brazil
Phone: (+5521) 2233 0288; dalvic@easyline.com.br

ABSTRACT

A mathematical model simulating the performance of a new rotary compressor is developed. An innovative driving mechanism imposes phased variable angular speeds to two concentric displacers, thus providing a volume variation in the gas compression spaces. A traditional simulation model for positive displacement compressors is employed, where mass and energy conservation equations, in differential form, are applied to the control volumes (two compression spaces). Uniformly distributed thermodynamic properties of gas, varying with time, are assumed for each control volume. Equations describing the volume variation with time, the gas to cylinder wall heat transfer and gas flow through valve ports and leakage passages are also employed. The resulting mathematical model is a system of ordinary differential equations, the numerical integration of which provides the time-history of pressure and temperature of the gas inside the compression chambers. A brief parametric analysis is carried out, showing the effect of geometry and operational parameters on the predicted performance of the compressor.

1. INTRODUCTION

Recent advances in the development program of an innovative rotary compressor (Kopelowicz, 2003) are presented in this paper. Rotary compressors are, of course, positive displacement machines where the traditional piston-slider crank mechanism of the reciprocating compressor is substituted by some sort of arrangement where the displacer (played by the piston in reciprocating compressors) presents a predominantly rotating movement. For this reason, rotary compressors are less subject to mechanical vibration and, for a given volumetric capacity, are usually smaller than their reciprocating counterpart. Different types of rotary compressors are now available, including the sliding vane, rolling piston, scroll and screw compressors, all of which have found commercial application in refrigeration and many other fields. This paper presents the development of a mathematical model that simulates the thermodynamic behavior of a new rotary positive displacement compressor. Since no similar machine has yet been constructed, the simulation model becomes an essential tool to establish basic geometric relations for the design and construction of a first prototype.

2. COMPRESSOR DESCRIPTION

Figure 1a depicts the schematics of the proposed compressor. Two displacers rotate concentrically, in an annular space, at variable and phased angular velocities, thus creating two variable-volume compression spaces between them. Each displacer is attached to its own rotor. The movement of the rotor/displacer assemblies is dictated by fixed-length levers pivoted to a common slot of a driving disk, Figure 1b, driven, by its turn, by a constant speed electric motor. The pivoting point of each displacer is allowed to slide along the driving disk slot, as shown in Figure 1a. The resulting movement of the displacers and their respective sliding pivot points (guides) is depicted in Figures 2a and 2b, showing displacer and guide positions at each 45-degree of the driving axis. The locations of the suction and discharge ports are also shown in Figure 2a.

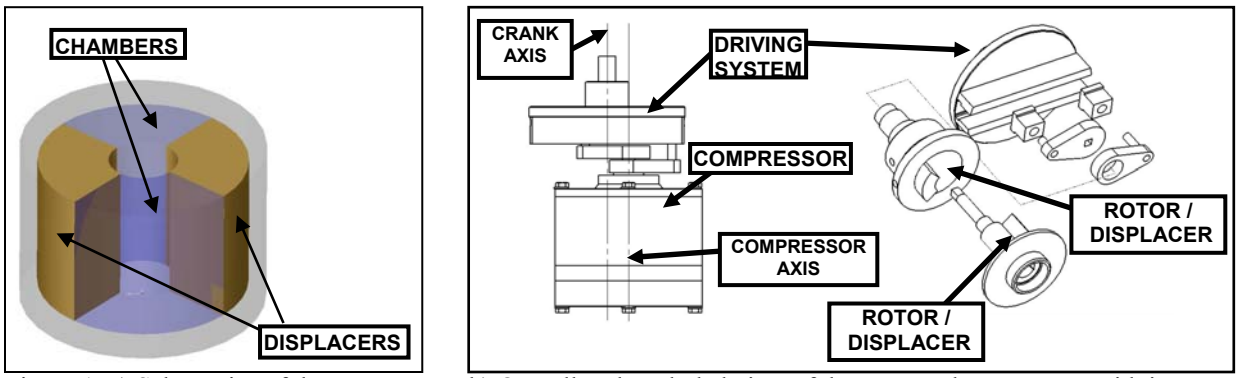

Figure 1: a) Schematics of the compressor. b) Overall and exploded view of the proposed compressor with its driving mechanism.

In spite of the guides (pivoting points) both translational and rotational movements, the levers are limited to rotate about the compressor axis. The angular velocity of the levers, and their respective rotor/displacer assemblies, is determined by the position of their pivoting points. If a guide is in the center of the disk, it will rotate around its own axis and will not rotate the lever. When it moves along the slot, it gains translational movement, which is converted to rotational movement when transmitted to the levers. The angular velocity increases when the guide moves farther away from the disk center and decreases when otherwise. This innovative mechanism, patented by Kopelowicz (2003), thus provides the required variable and phased angular velocity of the displacers. Inspection of Figure 2a shows that this is a positive displacement double-acting rotary compressor, with two full compression cycles per revolution of the driving axis. Suction and discharge ports, eventually with valves, must be strategically located at the circumference of the cylinder, in the valve plate.

The amplitude of the angular speed variation of the displacers is dictated by the eccentricity of the device, i.e., the distance between compressor and electric motor axes. If the compressor axis is aligned with driving plate axis, the distance from the lever guides to the disk center will be equal, thus imposing equal velocities to their displacers and producing no compression. When an eccentricity is added, that distance will be different, resulting in a 180 degree phased movement and chamber's volume variation. The eccentricity can be mechanically adjusted, allowing unique soft startups, with no compression and progressive increase of speed up to the required operating conditions. Soft startups contribute to extend equipment life and reduce maintenance costs. Also, capacity control systems could be implemented to modulate the compressor volumetric capacity, reducing energy consumption when lower capacity is required and maintaining continuous operation.

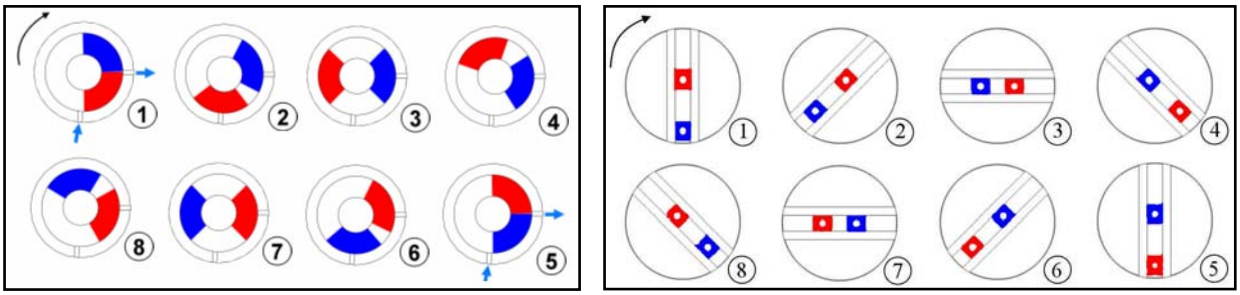

Figure 2: a) Displacers positioning at every 45 degrees for one full shaft revolution; b) Corresponding levers pivoting points positioning.

Figure 3 shows a section view of the compressor. Basic components are: rotors A and B, encompassing respective shafts, displacers A and B, firmly attached to their corresponding rotors, shell, top and lower covers, and the valve "plate", in fact a ring where suction and discharge gas passages are drilled radially and valves are installed. The discharge valve has to be positioned in the inner surface of the valve plate, to avoid excessive clearance volume. To be noted the concentric movement of both displacers, leading to an operation with lower vibration levels. Internal and external gas leakage can be diminished with proper manufacturing tolerances or with the use of seals.

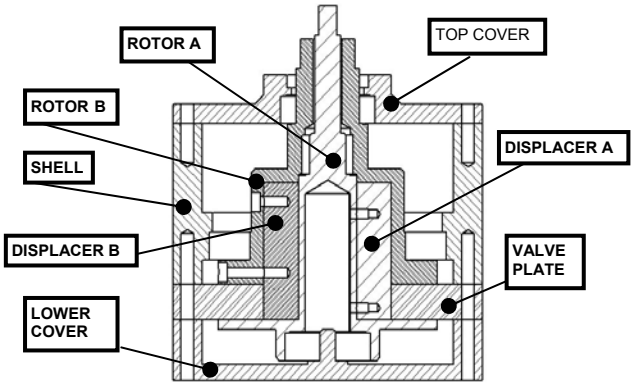

Figure 3: Section view of the compressor.

3. MATHEMATICAL MODEL

The traditional transient method (angle-by-angle) of simulating positive displacement compressors (Soedel, 1972; Ignatiev, 2000) was employed for compression of air. Two control volumes were established, comprising each one of the compression spaces (Figure 1b). Mass and energy conservation equations were applied assuming uniformly distributed gas properties in the control volume.

$$\frac{dm}{dt} = \sum_j \dot{m}_j \tag{1}$$

$$\frac{dE}{dt} = \dot{Q} - \frac{\delta W}{\delta t} + \sum_j \dot{m}_j i_j \tag{2}$$

Assuming perfect gas and negligible variation of the kinectic and potential energies, and combining Equations (1) and (2), the time-derivative of the gas temperature in the compression chamber is given by:

$$\frac{dT}{dt} = -\frac{1}{mc_v}\left\{-\dot{Q} + \sum_j \left[\dot{m}_j c_p (T - T_j)\right] + P\frac{dV}{dt} - RT\sum_j \dot{m}_j\right\} \tag{3}$$

3.1 Equations of motion: displacer position and angular velocity

Figure 4 shows the basic geometric parameters of the compressor, with displacers and drive mechanism.

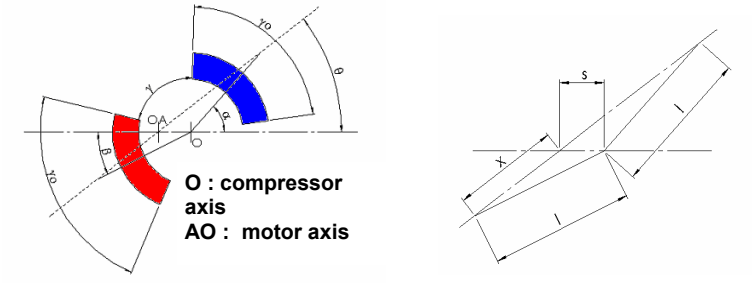

Figure 4: Geometric parameters of the displacers and driving mechanism.

Taking both levers horizontally opposed as the starting position ($\alpha = \beta = \theta = 0$, Figure 2a, frame [3]), the angular position of displacers B and A (phased by 180°) are given by, respectively:

$$\beta = \theta - arc\sin\left(\frac{s}{l}\sin\theta\right) = \theta - arc\sin(r\sin\theta) \;\; ; \;\; \alpha = 2\theta - \beta \tag{4}$$

The chamber angular clearance, i.e., the angular distance between the two displacers, is:

$$\gamma = \beta + \pi - \alpha - \gamma_0 \tag{5}$$

The time derivative of Equations (4) provides the instantaneous angular velocity of both displacers, as a function of the electric motor constant angular velocity, $\dot{\theta}$.

$$\dot{\beta} = \dot{\theta}\left(1 - \frac{(r\cos\theta)}{\sqrt{1 - r^2\sin^2\theta}}\right) \;\; ; \;\; \dot{\alpha} = 2\dot{\theta} - \dot{\beta} \tag{6}$$

Note that the second term inside the parenthesis gives the variation of the angular velocity around the constant value of the driving shaft speed, $\dot{\theta}$, and the amplitude of this variation is a function of the eccentricity ratio, $r = (s/l)$.

3.2 Volume Equation

The rate of change of the control volume is obtained from the angular clearance, γ.

$$\frac{dV}{dt} = \left(D_e^2 - D_i^2\right)\frac{L}{8}\frac{d\gamma}{dt} \tag{7}$$

3.3 Heat Transfer Rate Equation

Neglecting radiation, the heat exchange rate between the gas and control volume walls is given by:

$$\dot{Q} = hA_q(T_w - T) \tag{8}$$

where the total instantaneous heat exchange area, combining the six faces of the control volume, Figure 1a, is:

$$A_q = \frac{\left(D_e^2 - D_i^2\right)\gamma}{4} + \left(D_e - D_i\right)L + \frac{L\gamma}{2}\left(D_e + D_i\right) \tag{9}$$

The instantaneous heat transfer coefficient is adapted from a correlation originally developed for sliding-vane compressors (Gnutek e Kalinowski, 1996).

$$h = \frac{Nu\;\lambda}{l} \;\; ; \;\; Nu = C\left(\mathrm{Re}\right)^a\left(\mathrm{Pr}\right)^b \;\; ; \;\; \mathrm{Re} = \frac{\overline{w}\;l}{\upsilon} \tag{10}$$

Parameters *C*, *a* and *b* are, for laminar flow, 0.66, 0.6 and 0.33, respectively, and 0.037, 0.8 and 0.43, for turbulent flow. Transition is assumed to occur at $Re=10^5$. Reynolds number characteristic length and velocity are defined as:

$$l = \frac{\gamma\left(D_e + D_i\right)}{4} \quad ; \quad \overline{w} = \frac{\left|\dot{\beta} - \dot{\alpha}\right|\left(D_e + D_i\right)}{4} \tag{11}$$

3.4 Mass Flow Equations

Mass flow across the control surfaces, $\dot{m}_j$ in Equations (1) and (2), occurs through valve passages and leakage paths.

3.4.1.Valve Mass Flow Rate Equation. The compressor was modeled as having suction and discharge valves, both regarded as sharp-edged orifices, operating at fully-open/fully-closed position. Sub-sonic quasi-steady flow and upstream stagnation conditions were assumed. Mass flow rate was calculated from the isentropic flow expression, e.g., from Parise and Cartwright (1985), corrected by a discharge coefficient (Deschamps et al., 1988).

$$\dot{m}_v = C_d A_v \frac{P_1}{T_1^{1/2}} \left\{ \frac{2k}{R(k-1)} \left[\left(\frac{P_2}{P_1} \right)^{\frac{2}{k}} - \left(\frac{P_2}{P_1} \right)^{\frac{k+1}{k}} \right] \right\}^{1/2} \tag{12}$$

3.4.2 Mass Flow Rate through Leakage Paths. The relative movements between the displacers, rotors and valve plate require a clearance fit, so that leakage will occur between spaces (compression chambers, at pressures P_I and P_{II}, and shell space, at suction pressure). Gas leakage can occur from chamber to chamber (circumferential flow) and from chamber to shell space (radial and axial flow). Also, no leakage between rotors and their respective displacers due to adequate assembly sealing. Following experience with a prototype under construction, radial and axial leakage flows were neglected by the present model, due to the existence of appropriate seals.

As for circumferential flows, Figure 5 depicts possible leakage paths between compression chambers. To determine the tangential leakage, gas flow between parallel plates, one stationary and the other at a velocity U, is assumed, neglecting curvature effects and the presence of oil. Assuming constant pressure gradient, the leakage mass flow rate out of control volume I is given by (Fox and McDonald, 1998):

If $P_I - P_{II} > 0$:

$$\dot{m}_l = -\zeta \left[\frac{U\delta}{2} + \frac{1}{12\mu} \left(\frac{P_I - P_{II}}{\Delta z} \right) \delta^3 \right] \rho \tag{13}$$

If $P_I - P_{II} < 0$:

$$\dot{m}_l = \zeta \left[-\frac{U\delta}{2} + \frac{1}{12\mu} \left(\frac{P_I - P_{II}}{\Delta z} \right) \delta^3 \right] \rho \tag{14}$$

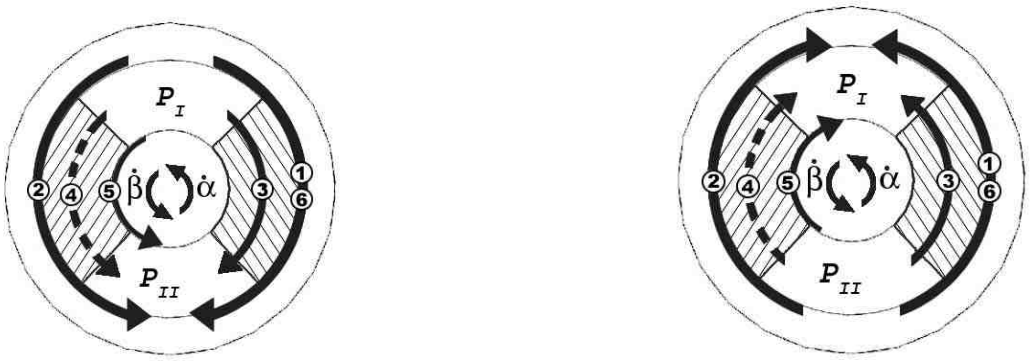

Figure 5: Possible leakage paths between compression spaces. a) (P_I-P_{II})>0; b) (P_I-P_{II})<0.

Two slightly different equations, (13) and (14), are necessary since both displacers rotate on the same direction but pressure difference between chambers, $(P_I - P_{II})$, oscillate between positive and negative. When the relative speed, U, is positive (direction from higher to lower pressure), it contributes to leakage flow and the opposite when negative. The parameters for equations (13) and (14) for different leakage paths are given on table 1.

Table 1: Leakage flow parameters.

LEAKAGE PATH (FIG. 5)	AVERAGE WIDTH	RELATIVE VELOCITY	AVERAGE DISTANCE
1- Lateral leakage between the valve plate and displacer A	$\zeta = L_a$	$U = -\dot{\alpha}\frac{D_e}{2}$	$\Delta z = \frac{\gamma_o D_e}{2}$
2- Lateral leakage between the valve plate and displacer B	$\zeta = L_a$	$U = -\dot{\beta}\frac{D_e}{2}$	$\Delta z = \frac{\gamma_o D_e}{2}$
3- Top leakage between rotor B and displacer A	$\zeta = \frac{D_e - D_i}{2}$	$U = -(\dot{\alpha} - \dot{\beta})\left(\frac{D_e + D_i}{4}\right)$	$\Delta z = \frac{D_e + D_i}{4}\gamma_o$
4- Lower leakage between rotor A and displacer B	$\zeta = \frac{D_e - D_i}{2}$	$U = (\dot{\alpha} - \dot{\beta})\left(\frac{D_e + D_i}{4}\right)$	$\Delta z = \frac{D_e + D_i}{4}\gamma_o$
5- Internal leakage between rotor A and displacer B	$\zeta = L$	$U = (\dot{\alpha} - \dot{\beta})\frac{D_i}{2}$	$\Delta z = \frac{\gamma_o D_i}{2}$
6- External leakage between rotor B and displacer A	$\zeta = L - L_a$	$U = -(\dot{\alpha} - \dot{\beta})\frac{D_e}{2}$	$\Delta z = \frac{\gamma_o D_e}{2}$

4. NUMERICAL METHOD

Equations (4) to (14) are substituted into Equation (3), to form, with Equation (1), a system of non-linear ordinary differential equations. Integration was performed by the Euler method, with time increments of one crank angle degree. To guarantee numerical stability, this increment was further refined whenever suction or discharge valves were open. Starting from an arbitrarily established thermodynamic state, the 360-degree compression cycle calculation was performed several times until convergence (pressure and temperature values at $\theta=0^o$ and $\theta=360^o$) was attained. Once one full cycle was performed, the pressure and temperature history of the chamber was phased by 180 degrees to describe the second chamber, thus allowing the leakage flow rates to be calculated.

5. RESULTS

The model was applied to simulate the compressor with the following input data: suction pressure – 100 kPa; suction temperature – 324.15 K; discharge pressure – 1 MPa; driving shaft angular velocity – 2000 rpm; cylinder width – 0.06 m; internal diameter – 0.038 m; external diameter – 0.088 m; displacers angle – 90^o; valve discharge coefficient – 0.48; valve passage diameter – 0.015 m; valve maximum displacement – 0.0015 m; gap (overall) – 0.03 mm. Figure 6 shows the predicted pressure-volume diagram for eccentricity ratios, ranging from 0.6 to 0.7. One can observe the effect that the eccentricity has on both maximum and minimum volumes of the compression space, notably the latter. This means that the eccentricity ratio alters both displaced volume, $(V_{\max} - V_{\min})$, and the clearance ratio, $V_{\min}$, which constitute a reasonable possibility for capacity control. Theoretically, from geometrical

considerations from Figure 4, the clearance volume could be brought to zero, although manufacturing tolerances required some clearance to avoid displacer contact.

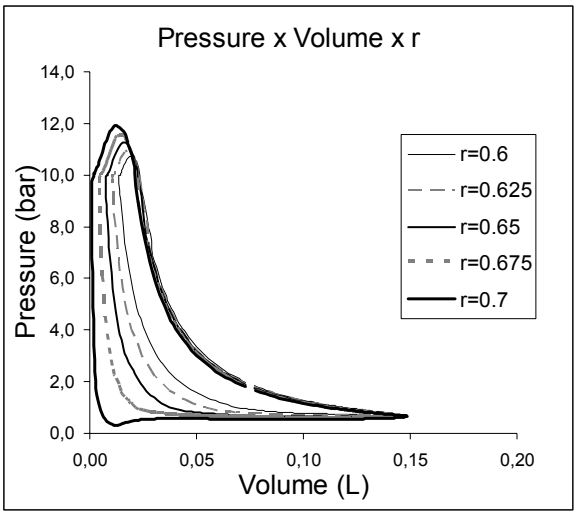

Figure 6: Pressure-Volume Diagram for different shaft eccentricity ratios.

6. CONCLUDING REMARKS

A new type of rotary compressor was proposed and simulated. Initial results, obtained from a simplified simulation model, have demonstrated the technical feasibility of the proposed positive displacement device. A first prototype was constructed to evaluate, at relatively low speeds, the behavior of the volume variation mechanism. Since no previous reference was available for this compressor, the simulation model proved to be an important tool in the design of a second prototype, which is presently under test, operating at realistic compressor operational conditions.

NOMENCLATURE

a	exponent in Equation (10)
A	area (m^2)
b	exponent in Equation (10)
c_p	specific heat at constant pressure (J/kgK)
c_v	specific heat at constant volume (J/kgK)
C	constant in in Equation (10)
C_d	discharge coefficient (-)
D_e	displacer external diameter (m)
D_i	displacer internal diameter (m)
E	energy (J)
h	heat transfer coefficient (W/m^2K)
i	specific enthalpy (J/kg)
l	characteristic length (m)
k	specific heat ratio (-)
L	displacer width (m)
m	mass (kg)
$\dot{m}$	mass flow rate (kg/s)
Nu	Nusselt number (-)
P	pressure (Pa)
Pr	Prandtl number (-)
R	gas constant (J/kgK)
r	eccentricity ratio (-)
Re	Reynolds number (-)
$\dot{Q}$	rate of heat transfer (W)
s	eccentricity (m)
t	time (s)
T	temperature (K)
U	relative velocity (m/s)
V	volume (m^3)
$\overline{w}$	characteristic velocity (rad/s)
W	work (J)
Δz	average length of leakage path (m)

Greek Symbols

α	angular position of displacer A (rad)
$\dot{\alpha}$	angular velocity of displacer A (rad/s)
β	angular position of displacer B (rad)
$\dot{\beta}$	angular velocity of displacer B (rad/s)

δ	gap (m)
γ	angular clearance (rad)
γ_0	displacer angle (rad)
θ	driving shaft angle (rad)
$\dot{\theta}$	driving shaft angular velocity (rad/s)
λ	thermal conductivity (W/mK)
μ	viscosity (kg/m.s)
υ	kinematic viscosity (m^2/s)
ρ	density (kg/m^3)
ζ	leakage path average width (m)

Subscripts

1	upstream
2	downstream
I	relative to control volume I
II	relative to control volume II
j	j^{th} flow passage across the control volume
l	leakage
q	heat transfer
v	valve
w	wall

REFERENCES

Deschamps, C.J., Ferreira, R.T.S, Prata, A.T., 1988, "The Effective Flow and Force Areas in Compressor Valves", 1988 International Compressor Engineering Conference At Purdue, Purdue University, July 18-21, West Lafayette, USA.

Fox, R.W., McDonald, A.T., 1998, Introduction to Fluid Mechanics, John Wiley & Sons.

Gnutek, Z., Kalinowski, E., 1996, "Heat Exchange in the Working Chamber of a Multi-vane Compressor", 1996 International Compressor Engineering Conference at Purdue, Purdue University, vol II, July 23-26, West Lafayette, USA.

Ignatiev, K., 2000, Compressor Modeling, USC/IIR Short Course "Simulation tools for vapor compression systems and component analysis", Purdue University, July 23-24, West Lafayette, USA.

Kopelowicz, H.J., 2003, "A system for the construction of pumps, compressors and motor engines, formed by a rotary chamber and pistons which are driven in the same direction at varying velocities alternatively opposite to each other, inside a fixed open or closed structure", International Patent Application under PCT, International Publication Number WO 03/014549 A1, 20 February.

Parise, J.A.R., Cartwright, W.G., 1985, "Simulation of Reciprocating Compressors: Numerical Method and Comparison with Experimental Data", *Revista Brasileira de Ciências Mecânicas*, VII (2), pp. 129-152.

Soedel, W., 1972, "Introduction to Computer Simulation of Positive Displacement Type Compressors", 1972 Short Course Text, Ray W. Herrick Laboratories, School of Mechanical Engineering, Purdue University, West Lafayette, USA.

ACKNOWLEDGEMENTS

Thanks are due to FINEP, CAPES and CNPq, Brazilian research agencies, which have financially supported this work.